Synthesis and characterisation of $Y_2O_3:Bi^{3+}$ phosphor material

E Lee, HC Swart, JJ Terblans

Department of Physics, University of the Free State, PO Box 339, Bloemfontein, 9300, South Africa

Email: LeeE@ufs.ac.za, SwartHC@ufs.ac.za, TerblansJJ@ufs.ac.za

Abstract. Bismuth doped yttrium oxide ($Y_2O_3:Bi^{3+}$) phosphor was synthesised using co-precipitation method. During synthesis, the pH value and Bi^{3+} concentration were varied to study their effects on the luminescent properties of the phosphor. X-ray diffraction patterns showed the phosphor samples had retained its single-phase cubic structure. The crystallite size was determined using the Scherrer equation, which showed that crystallite size was more dependent on the pH during synthesis than that of Bi ion concentration. The photoluminescence spectra revealed two strong excitation bands centred at 330 nm and 390 nm, along with two emission bands one centred at 409 nm and another broad band centred at 489 nm which corresponds to the two sites within the host matrix where Bi ions may occupy. By monitoring the 489 nm emission band intensity, it revealed that the variations in the pH value during synthesis had influenced the luminescent intensity of the phosphor. Altering the Bi^{3+} concentration in the Y_2O_3 host material also influenced the emission intensity of the phosphor, where the maximum intensity was found when the phosphor was synthesised at pH 10 with a Bi^{3+} concentration of 2.0 mol%.

1. Introduction

Solar energy is the most abundant and cleanest source of energy currently available. This led to the invention of photovoltaic (PV) solar cells capable of converting solar energy into electrical energy. Solar cells fabricated from single junction crystalline silicon (c-Si) is the most widely used PV cell but suffers from an efficiency limit of round 29 % [1]. The low conversion efficiency from solar energy to electrical energy results from the mismatch between the solar spectrum and the absorption spectrum of c-Si where the strongest spectral response of c-Si solar cells is around 1000 nm [2-4].

In the past decade, luminescent materials doped with rare-earth elements have been used extensively in the lighting industry, due to the wide range of possible luminescence from ultraviolet (UV) through the visible to the near-infrared (NIR) regions [5, 6]. RE^{3+}-Yb^{3+} (RE = Tb, Ce, Er and Pr) co-doped phosphors are of great interest for down-converting UV photons to NIR photons, used to improve the efficiency of solar cells [7]. Yb^{3+} serves as a suitable acceptor ion as it contains only a single excitation state correlating to an emission at around 1000 nm, very close to the maximum absorption efficiency of c-Si [8, 9]. Lanthanides or rare-earth metals are generally poor at absorbing photons in the UV to blue regions due to their parity forbidden 4f transition [10]. Thus more attention has been placed on metal ions as possible alternatives to the current rare-earth sensitisers [2, 11]. Metal ions such as Bi^{3+} which have a $6s^2$ electron configuration making the $6s^2 \rightarrow 6s6p$ transition an allowed transition [12]. This allowed transitions present in Bi gives rise to much broader excitation and emission bands as compared to rare-earths which are generally narrower [13]. Y_2O_3 phosphor doped with Bi^{3+} ions show a strong emission band between 490 and 510 nm when exposed to UV light [2, 12, 14]. The energy associated

with the visible emission of Bi^{3+} is twice the energy required for the $^2F_{7/2} \rightarrow {}^2F_{5/2}$ transition of Yb^{3+} and indicates that cooperative energy transfer (CET) from Bi^{3+} to Yb^{3+} could occur [15].

In this study $Y_2O_3:Bi^{3+}$ phosphors were prepared using co-precipitation under different pH values and Bi^{3+} concentrations to investigate their effects on the particle sizes and the luminescent properties.

2. Experimental

2.1. Synthesis of $Y_{2-x}O_3:Bi_x$

$Y_2O_3:Bi^{3+}$ powder phosphor was prepared using the co-precipitation method under various pH values and different doping concentrations. Y_2O_3 (99.99%) and Bi_2O_3 (99.9%) were used as the starting reagents. Stoichiometric amounts of Y_2O_3 and Bi_2O_3 were dissolved in concentrated nitric acid (HNO_3) through heating and stirring until an aqueous solution consisting of $Y(NO_3)_3$ and $Bi(NO_3)_3$ was obtained. Once the starting material has completely dissolved ammonia (NH_4OH) was added to the acid solution, under vigorous stirring to maintain a pH from 6 to 10 and stirred for a further 2 hours. The white precipitate was collected then washed using ethanol to remove any unreacted materials. The product was placed in an oven at 80 ºC for at least 12 hours to evaporate the ethanol that was introduced during washing. Using a mortar, the dried mass was crushed before being placed in an annealing furnace for 1 hour at 450 ºC and finally at 1000 ºC for 2 hours.

The effect of pH on the luminescence properties of $Y_2O_3:Bi^{3+}$ phosphors were investigated using a spectrometer and showed that samples synthesised under pH 10 displayed the strongest luminescence. Thus all further phosphors were synthesised with pH 10.

2.2. Characterisation

The crystal structure of the powder samples was characterised from x-ray diffraction (XRD) measurements using a Bruker D8 Advance diffractometer with KαCu x-rays (1.54 Å). The emission and excitation properties of the $Y_{2-x}O_3:Bi_x$ phosphor samples were measured using a Varian Cary Eclipse fluorescence spectrophotometer.

3. Results and discussion

The XRD pattern for $Y_{1.98}O_3:Bi_{2.0\%}$ prepared under different pH conditions are represented in figure 1(a), while figure 1(b) shows the (222) peak shifts of phosphors prepared at different pH values.

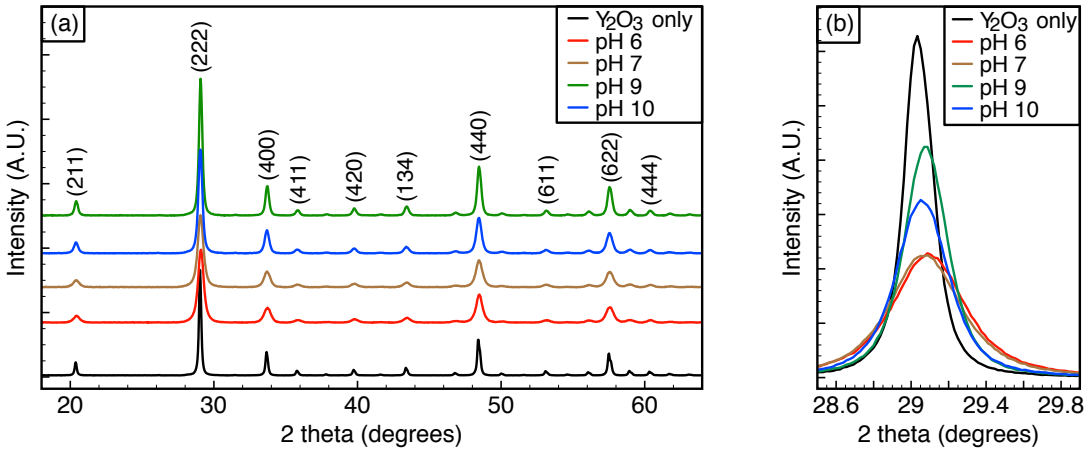

Figure 1 (a) XRD pattern of $Y_{1.98}O_3:Bi_{2.0\%}$ phosphor powder synthesised at pH 6, 7, 9 and 10 along with non-doped Y_2O_3 starting material. (b) The (222) peak shift of $Y_{1.98}O_3:Bi_{2.0\%}$ phosphor as compared to non-doped Y_2O_3.

The measure XRD patterns correlates wells to that of the non-doped Y_2O_3 starting material. From the XRD patterns, it showed that varying the pH value during synthesis did not alter the crystal structure

of the host material as it still resembles a single phase cubic structure. The absence of any additional diffraction peaks suggests that no impurity phases were present. Thus shifts can be attributed to the addition of Bi ions which caused stress and strain within the host matrix.

Figure 2(a) shows both the excitation and emission spectra of a $Y_{1.98}O_3$:$Bi_{2.0\%}$ phosphor synthesised at pH 6. An illustration of the two occupational site with the Y_2O_3 host matrix is shown in figure 2(b).

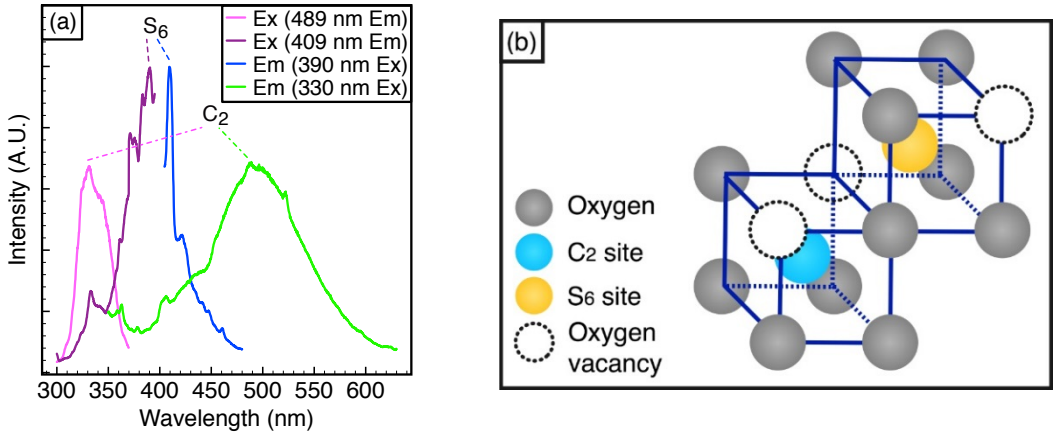

Figure 2: (a) Excitation and emission spectra of $Y_{1.98}O_3$:$Bi_{2.0\%}$ phosphor due to the C_2 and S_6 occupational sites of Bi ions. (b) Schematic illustration of the C_2 and S_6 sites in cubic Y_2O_3.

Using an excitation wavelength λ_{ex} = 330 nm an emission spectrum showing a strong green emission at 489 nm was observed. When exciting at λ_{ex} = 390 nm a strong blue emission situated at 409 nm was measured. For emission λ_{em} = 489 nm an excitation band was obtained with the maximum located at 330 nm. Similarly observing at an emission wavelength λ_{em} = 409 nm an excitation spectrum yielded three excitation bands one located at 330 nm, the second at 370 nm and the strongest peak at 390 nm. The existence of the two emission (409 nm and 489 nm) and excitation (330 nm and 390 nm) bands were a direct result of the two possible sites that the Bi^{3+} ions are able to occupy in the Y_2O_3 host matrix. The emission and excitation bands centred at 489 nm and 330 nm respectively is responsible for the excitation and emission of the Bi^{3+} ion situation in the C_2 site where as the S_6 site correlates to the 409 nm emission and 390 nm excitation bands [2, 11, 16].

Figure 3(a) shows the 489 nm emission and 330 nm excitation spectra of $Y_{1.98}O_3$:$Bi_{2.0\%}$ phosphor prepared at pH 6, 7, 9 and 10. The effect of pH on the 489 nm emission intensity is shown in figure 3(b).

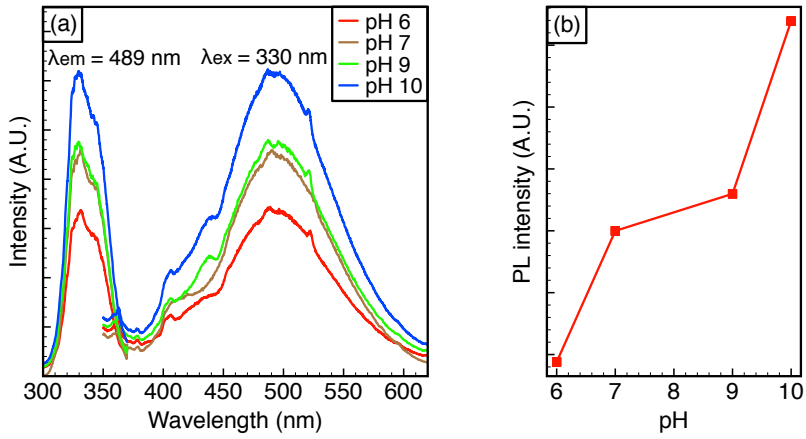

Figure 3: (a) The 330 nm excitation and 489 nm emission spectrum for $Y_{1.98}O_3$:$Bi_{2.0\%}$ synthesised at varying pH values. (b) PL intensity of 489 nm emission as a function of pH.

While monitoring the emission wavelength λ_{em} = 489 nm, similar to the sample prepared at pH 6, a broad and intense band centred at 330 nm was observed. Additionally, when the phosphor samples were excited at λ_{ex} = 330 nm a broad emission band with maximum at around 489 nm was observed. The outer most $6s^2$ electron configuration of Bi^{3+} houses one energy level $^1S_0$ (ground state) and while in the 6s6p configuration (excited state) it splits into four levels $^3P_0$, $^3P_1$, $^3P_2$ and $^1P_1$ in order of increasing energy. Due to the Δj selection rule, transitions from $^1S_0 \rightarrow {}^3P_1$ and $^1S_0 \rightarrow {}^1P_1$ are allowed transitions whereas transitions $^1S_0 \rightarrow {}^3P_0$ and $^1S_0 \rightarrow {}^3P_2$ are strictly forbidden. Thus the excitation band at 330 nm and emission band at 489 nm are attributed to the transition from $^1S_0 \rightarrow {}^3P_1$ and $^3P_1 \rightarrow {}^1S_0$ respectively [2, 17-19].

It can be seen in figure 3 that emission intensity vary sufficiently with variations in the pH with the strongest emission intensity found when the $Y_{1.98}O_3$:$Bi_{2.0\%}$ phosphor was synthesised at pH 10, therefore further synthesis was conducted at pH 10.

The XRD results for the $Y_{2-x}O_3$:Bi_x phosphor prepared at varying Bi ion concentrations and at pH 10 are shown in figure 4(a). The results show a single phase cubic structure similar to the structure found when varying pH and the absence of additional peaks shows that no impurity phases had been introduced. The shifts in the main (222) peak shown in figure 4(b) of the cubic structure were due to the stress and strain present in the crystal when Bi ions were introduced into the host matrix.

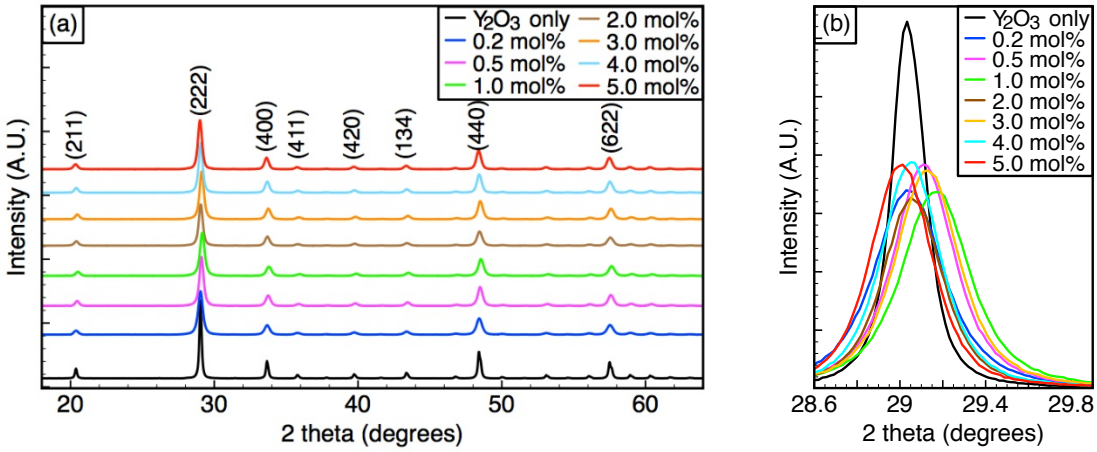

Figure 4: (a) XRD patterns for $Y_{2-x}O_3$:Bi_x (x = 0.2, 0.5, 1.0, 2.0, 3.0, 4.0 and 5.0 mol%) phosphor synthesised using pH 10. (b) The (222) peak shift due to the addition of Bi ions.

The effect of varying pH and Bi concentrations on the crystallite size are shown in figure 5. The crystallite sizes were calculated using the Scherrer equation (1) [20, 21].

$$\tau = \frac{K\lambda}{\beta \cos\theta} \tag{1}$$

τ is the crystallite size, K is the shape factor which has a typical value of 0.9, λ is wavelength of the X-ray used, β is the width of the peak at half its maximum intensity (FWHM) subtracted by the instrumental broadening (measured in radians) and θ is the Bragg angle. To obtain a better approximation of the crystallite size for each sample, all diffraction peaks indexed in Figure 1(a) and 4(a) were used and the average crystallite size for each sample was taken. The Scherrer equation revealed that changes in pH did indeed affect the crystallite size where the crystallite size increased with an increase in pH until a maximum at pH 9 where the size then decreased. In the case of varying Bi concentrations, the crystallite sizes were found to be similar ranging between 21 to 25 nm with no distinct pattern. This suggests that the crystallite size was more dependent on the pH during synthesis than the concentration of Bi dopants.

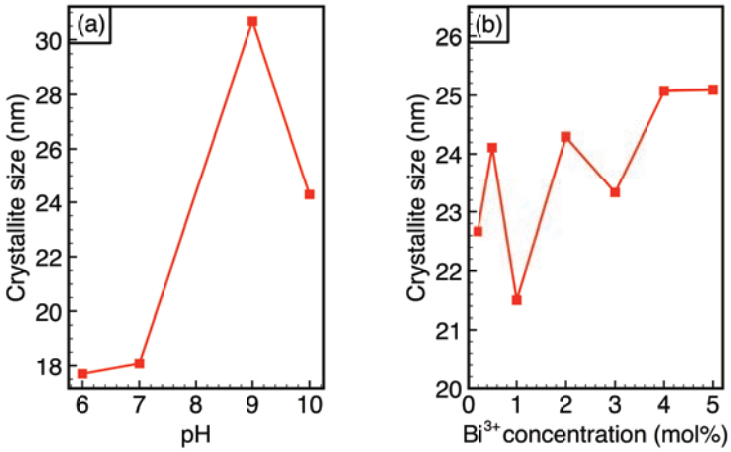

Figure 5: (a) The effect of crystallite size due to the variations in pH during synthesis. (b) Crystallite size as a function of Bi concentration.

The 330 nm excitation and 489 nm emission spectra for varying Bi ion concentrations are represented in figure 6(a). The results showed that the luminescent intensity was also dependant on the Bi ion concentration as shown in figure 6(b).

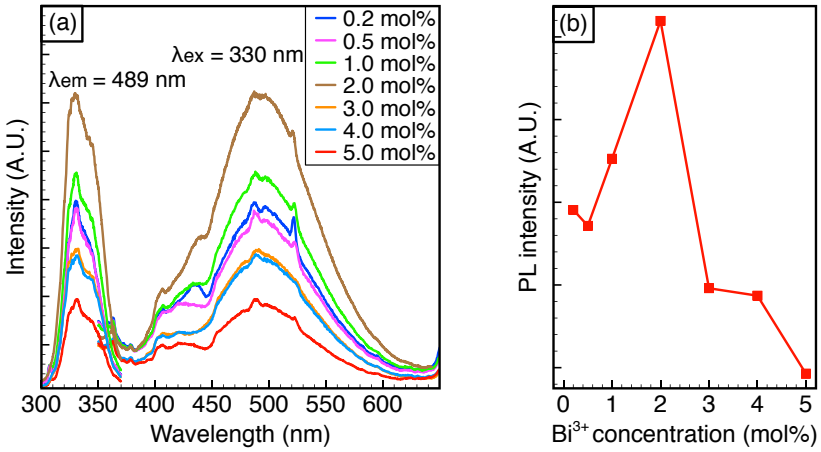

Figure 6: (a) Excitation and emission spectrum for $Y_{2-x}O_3$:Bi_x phosphor synthesised at varying Bi concentration. (b) PL intensity of 489 nm as a function Bi concentration.

Figure 6 showed that variations in Bi ion concentration does influence the luminescence intensity of the phosphor. Between 0.5 to 2.0 mol% Bi the luminescence increased with an increase in Bi concentration. The luminescent intensity then suddenly decreased between 3.0 to 5.0 mol% Bi. The sharp decrease in intensity was largely due to concentration quenching. Thus the strongest luminescence observed for the $Y_{2-x}O_3$:Bi_x phosphor was when the phosphor was synthesised at pH 10 and containing a Bi ion concentration of 2.0 mol%.

4. Conclusion

The Y_2O_3:Bi phosphor was successfully synthesised using the co-precipitation method. XRD patterns showed that variations in both the pH and Bi ion concentration did not influence the single phase crystal structure of the Y_2O_3 host material. Utilising the Scherrer equation it revealed that the pH during

synthesis has the strongest influence on the crystallite size of the final phosphor as compared to varying the Bi ion concentration. Photoluminescence showed the two-excitation and emissions bands, which corresponds to the two possible sites (C2 and S6) that Bi ions are able to occupy within the host matrix. While monitoring the 489 nm emission peak it showed that the luminescent intensity was influenced by the pH during synthesis, where an increase in pH showed an increase in the luminescent intensity of the phosphor. The influence of Bi concentration was also demonstrated by observing the 489 nm emission peak, which showed that increasing the Bi ion concentration also lead to an increase in the luminescent intensity until an ion concentration of 2.0 mol%. Thereafter any further increase in the Bi concentration a decrease in the 489 nm emission intensity was observed, due to the effect of concentration quenching. Thus the strongest luminescence was achieved when the $Y_{2-x}O_3$:Bi_x phosphor was synthesised at pH 10 with an Bi concentration of 2.0 mol%.

Acknowledgments
This research paper is made possible thanks to Prof HC Swart for his guidance through this project, to Prof RE Kroon for his input during PL measurements and Dr S Cronjé for his help in XRD measurements. Funding support is acknowledged to the South African Research Chairs Initiative of the Department of Science and Technology (DST) and the National Research Fund (NRF).

References

[1] Tiedje T, Yablonovitch E, Cody G D and Brooks B G 1984 *IEEE Transactions on Electron Devices* **31** 711
[2] Huang X Y, Ji X H and Zhang Q Y 2011 *Journal of the American Ceramic Society* **94** 833
[3] Saritas M and McKell H D 1987 *Journal of Applied Physics* **61** 4923
[4] Poruba A, Fejfar A, Remeš Z, Špringer J, Vanecek M, Kocka J, Meier J, Torres P and Shah A 2000 *Journal of Applied Physics* **88** 148
[5] Feldmann C, Jüstel T, Ronda C and Schmidt P 2003 *Advanced Functional Materials* **13** 511
[6] Richards B 2006 *Solar Energy Materials and Solar Cells* **90** 1189
[7] Trupke T, Green M A and Würfel P 2002 *Journal of Applied Physics* **92** 1668
[8] Li J, Zhang J, Zhang X, Hao Z and Luo Y 2014 *Journal of Alloys and Compounds* **583** 96
[9] Gao G, Peng M and Wondraczek L 2014 *J. Mater. Chem. C* **2** 8083
[10] Zhang Q and Huang X 2010 *Progress in Materials Science* **55** 353
[11] Rambabu U and Han S D 2013 *Ceramics International* **39** 1603
[12] Jacobsohn L G, Blair M W, Tornga S C, Brown L O, Bennett B L and Muenchausen R E 2008 *Journal of Applied Physics* **104** 124303
[13] Sun H, Zhou J and Qiu J 2014 *Progress in Material Science* **64** 1
[14] van de Craats A M and Blasse G 1995 *Chemical Physics Letters* **243** 559
[15] Xian-Tao W, Jiang-Bo Z, Yong-Hu C, Min Y and Yong L 2010 *Chinese Physics B* **19** 77804
[16] Avram D, Cojocaru B, Florea M and Tiseanu C 2016 *Opt. Mater. Express* **6** 1635
[17] Takeshita S, Isobe T, Sawayama T and Niikura S 2009 *Journal of Luminescence* **129** 1067
[18] Ilmer M, Grabmaier B C and Blasse G 1994 *Chemistry of Materials* **6** 204
[19] Kumar V, Kumar R, Lochab S and Singh N 2007 *Nuclear Instruments and Methods in Physics Research Section B: Beam Interactions with Materials and Atoms* **262** 194
[20] Scherrer P 1918 *Göttinger Nachrichten Math. Phys* **2** 98
[21] Monshi A, Foroughi M and Monshi M 2012 *World Journal of Nano Science and Engineering* **2** 154